arXiv:1510.01705v1 [cs.SY] 6 Oct 2015

Baseband Equivalent Models Resulting From Dynamic Continuous-Time Perturbations In Phase-Amplitude Modulation-Demodulation Schemes *

Omer Tanovic †, Alexandre Megretski†, Yan Li ‡,
Vladimir M. Stojanovic §, and Mitra Osqui ¶

October 7, 2015

Abstract

We consider discrete-time (DT) systems S in which a DT input is first transformed to a continuous-time (CT) format by phase-amplitude modulation, then modified by a nonlinear CT dynamical transformation F, and finally converted back to DT output using an ideal de-modulation scheme. Assuming that F belongs to a special class of CT Volterra series models with fixed degree and memory depth, we provide a complete characterization of S as a series connection of a DT Volterra series model of fixed degree and memory depth, and an LTI system with special properties. The result suggests a new, non-obvious, analytically motivated structure of digital compensation of analog nonlinear distortions (for example, those caused by power amplifiers) in digital communication systems. We also argue that this baseband model, and its corresponding digital compensation structure, can be readily extended to OFDM modulation. Results from a MATLAB simulation are used to demonstrate effectiveness of the new compensation scheme, as compared to the standard Volterra series approach.

*This work was supported by DARPA Award No. W911NF-10-1-0088. Shorter version of this paper was published in the proceedings of the European Control Conference 2015 [28]

†Omer Tanovic and Alexandre Megretski are with the Laboratory for Information and Decision Systems, Department of Electrical Engineering and Computer Science, Massachusetts Institute of Technology, Cambridge, MA 02139, USA {otanovic,ameg}@mit.edu

‡Yan Li was with the Research Laboratory of Electronics, Department of Electrical Engineering and Computer Science, Massachusetts Institute of Technology. Currently she is with NanoSemi Inc., Waltham, MA 02451, USA yan.li@nanosemitech.com

§Vladimir M. Stojanovic is with the Department of Electrical Engineering and Computer Sciences, University of California Berkeley, Berkeley, CA 94720, USA vlada@berkeley.edu

¶Mitra Osqui was with the Laboratory for Information and Decision Systems, Department of Electrical Engineering and Computer Science, Massachusetts Institute of Technology. Currently she is a Research Scientist at Lyric Labs — Analog Devices, Cambridge, MA 02142, USA mitra.osqui@analog.com

Key Words: communication system nonlinearities, nonlinear systems, modeling, phase modulation, amplitude modulation

1 Notation and Terminology

j	a fixed square root of -1
$\mathbb{C}$	complex numbers
$\mathbb{R}$	real numbers
$\mathbb{Z}$	integers
$\mathbb{N}$	positive integers
$[n]$	all positive integers from 1 to n
$[n]^d$	$= \underbrace{[n] \times [n] \times \cdots \times [n]}_{d-\text{times}}$, where $d \in \mathbb{N}$
$\mathcal{L}(X)$	bounded square integrable functions $\mathbb{R} \to X \subset \mathbb{C}$
$\mathcal{L}[X]$	2π-periodic square integrable functions $\mathbb{R} \to X \subset \mathbb{C}$
$\ell(X)$	square summable functions $\mathbb{Z} \to X \subset \mathbb{C}^n$
$\lvert S \rvert$	cardinality of the set S

CT signals are elements of $\mathcal{L}$, *DT signals* are elements of $\ell(X)$ for some $X \subset \mathbb{C}^n$. For $w \in \ell(X)$, $w[n]$ denotes the value of w at $n \in \mathbb{Z}$. In contrast, $x(t)$ refers to the value of $x \in \mathcal{L}$ at $t \in \mathbb{R}$. *Systems* are viewed as functions $\mathcal{L} \to \mathcal{L}$, $\mathcal{L} \to \ell(X)$, $\ell(X) \to \mathcal{L}$, or $\ell(X) \to \ell(Y)$. $\mathbf{G}f$ denotes the response of system $\mathbf{G}$ to signal f (even when $\mathbf{G}$ is not linear), and the *series composition* $\mathbf{K} = \mathbf{Q}\mathbf{G}$ of systems $\mathbf{Q}$ and $\mathbf{G}$ is the system mapping f to $\mathbf{Q}(\mathbf{G}f)$. A DT (or CT) LTI system $\mathbf{H}$ with *frequency response* $H \in \mathcal{L}[\mathbb{C}]$ (or $H \in \mathcal{L}(\mathbb{C})$ for CT) maps signal $x \in \ell(\mathbb{C})$ (or $x \in \mathcal{L}(\mathbb{C})$ for CT) to signal $y \in \ell(\mathbb{C})$ (or $y \in \mathcal{L}(\mathbb{C})$ for CT) such that $Y = HX$, where $X = \mathcal{F}(x)$, $Y = \mathcal{F}(y)$.

2 Introduction

In modern communications systems, with a demand for high-throughput data transmission, requirements on the system linearity become more strict. This is in large part due to a combination of ever increasing signalling rates with use of more complex modulation/demodulation schemes for enhanced spectral efficiency. This in turn forces RF transmitter power amplifiers (PA) to operate over a large portion of their transfer curves, generating out of band spectral content which degrades spectral efficiency. A common way to make the PA (and correspondingly the whole signal chain) behave linearly is to back-off PA's input level, which results in reduced power efficiency. Hence a need for a method which would help both increase linearity and power efficiency. Digital compensation offers an attractive approach to designing electronic devices with superior characteristics, and it is not a surprise that it has been used in this context as well. Nonlinear distortion in the analog system can be compensated with a predistorter or a compensator system. This predistorter inverts nonlinear behavior of the analog part, and is usually realized

with a digital system. Techniques which employ such systems are called digital predistortion (DPD) techniques, and they can produce highly linear transmitter circuits [1]-[3].

First attempts to mitigate PA's nonlinear effects by employing DPD involved using simple memoryless models in order to describe PA's behavior [4]. As the signal bandwidth has increased over time, it has been recognized that short and long memory effects play significant role in PA's behavior [5], and should be incorporated into the model. Since then several memory baseband models and corresponding predistorters have been proposed to compensate memory effects: memory polynomials [6, 7], Hammerstein and Wiener models [8], pruned Volterra series [9], generalized memory polynomials [10], dynamic deviation reduction-based Volterra models [11, 12], as well as the most recent neural networks based behavioral models [13], and generalized rational functions based models [14]. These papers emphasize capturing the whole range of the output signal's spectrum, which is proportional to the order of nonlinearity of the RF PA, and is in practice taken to be about five times the input bandwith. In wideband communication systems this would make the linearization bandwidth very large and would put a significant burden on the system design (e.g. it would require very high-speed data converters). Since these restrictions limit applicability of conventional models in the forthcoming wideband systems (e.g. LTE-advanced), it is beneficial to investigate model dynamics when the PA's output is also limited in bandwidth. In that case DPD would ideally mitigate distortion in that frequency band, and possible adjacent channel radiation could be taken care of by applying bandpass filter to the PA's output. Such band-limited baseband model and its corresponding DPD were investigated in [15], and promising experimental results were shown. Theoretical analysis shown in [15] follows the same modeling approach as the conventional baseband models (dynamic deviation reduction-based Volterra series modeling). Due to the bandpass filtering operation applied on the PA output, long (possibly infinite) memory dynamic behavior is now present, which makes these band-limited models fundamentally different from the conventional baseband models. Hence standard modeling methods, such as memory polynomials or dynamic deviation reduction-based Volterra series modeling, might be too general to pinpoint this new structure, and also not well suited for practical implementations (long memory requirements in nonlinear models would require exponentially large number of coefficients).

In this paper, we develop an explicit expression of the equivalent baseband model, when the passband nonlinearity can be described by a Volterra series model with fixed degree and memory depth. We show that this baseband model can be written as a series connection of a fixed degree and low memory Volterra model, and a long memory discrete LTI system which we call the reconstruction filter. These filters exibit discontinuities at frequency values $\pm\pi$, making their unit step responses very long (possibly infinitely long). Despite this undesirable property, they are shown to be smooth over the interval $(-\pi, \pi)$, and thus aproximable by low order polynomials. This result suggests a new, non-obvious, analytically motivated structure of digital precompensation of RF PA nonlinearities.

This paper is organized as follows. In Section III we further discuss motivation for considering problem of digital predistortion and give mathematical description of the system under consideration. Main result is stated and proven in Section IV, i.e. in this section we give an explicit expression of the equivalent baseband model. In Section V we provide some further discussion on advantages of the proposed method, and its extension to OFDM modulation.

DPD design and its performance are demonstrated by the MATLAB simulation results, and presented in Section VI. Finally we conclude the paper in Section VII.

3 Motivation and Problem Setup

In this paper, a digital compensator is viewed as a system $\mathbf{C}:\ \ell(\mathbb{R}) \to \ell(\mathbb{R})$. More specifically, a *pre*-compensator $\mathbf{C}:\ \ell(\mathbb{R}) \to \ell(\mathbb{R})$ designed for a device modeled by a system $\mathbf{S}:\ \ell(\mathbb{R}) \to \mathcal{L}$ (or $\mathbf{S}:\ \ell(\mathbb{R}) \to \ell(\mathbb{R})$) aims to make the composition $\mathbf{SC}$, as shown on the block diagram below,

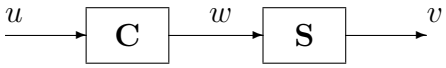

conform to a set of desired specifications. (In the simplest scenario, the objective is to make $\mathbf{SC}$ as close to the identity map as possible, in order to cancel the distortions introduced by $\mathbf{S}$.)

A common element in digital compensator design algorithms is selection of *compensator structure*, which usually means specifying a finite sequence $\tilde{\mathbf{C}} = (\mathbf{C}_1, \dots \mathbf{C}_N)$ of systems $\mathbf{C}_k:\ \ell(\mathbb{R}) \to \ell(\mathbb{R})$, and restricting the actual compensator $\mathbf{C}$ to have the form

$$\mathbf{C} = \sum_{k=1}^{N} a_k \mathbf{C}_k, \qquad a_k \in \mathbb{R},$$

i.e., to be a linear combination of the elements of $\tilde{\mathbf{C}}$. Once the *basis* sequence $\tilde{\mathbf{C}}$ is fixed, the design usually reduces to a straightforward *least squares optimization* of the coefficients $a_k \in \mathbb{R}$.

A popular choice is for the systems $\mathbf{C}_k$ to be some *Volterra monomials*, i.e. to map their input $u = u[n]$ to the outputs $w_k = w_k[n]$ according to the polynomial formulae

$$w_k[n] = \prod_{i=1}^{d_r(k)} \text{Re}\, u[n - n^r_{k,i}] \prod_{i=1}^{d_i(k)} \text{Im}\, u[n - n^i_{k,i}]$$

(where the integers $d_r(k)$, $d_i(k)$, $n^r_{k,i}$, $n^i_{k,i}$ will be referred to, respectively, as the *degrees* and *delays*), which makes every linear combination $\mathbf{C}$ of $\mathbf{C}_k$ a *DT Volterra series* [17], i.e., a DT system mapping signal inputs $u \in \ell(\mathbb{C})$ to outputs $w \in \ell(\mathbb{C})$ according to the polynomial expression

$$w[n] = \sum_{k=1}^{N} a_k \prod_{i=1}^{d_r(k)} \text{Re}\, u[n - n^r_{k,i}] \prod_{i=1}^{d_i(k)} \text{Im}\, u[n - n^i_{k,i}].$$

Selecting a proper *compensator structure* is a major challenge in compensator design: a basis which is too simple will not be capable of cancelling the distortions well, while a form that is too complex will consume excessive power and space. Having an insight into the compensator basis selection can be very valuable. For an example (cooked up outrageously to make the point), consider the case when the ideal compensator $\mathbf{C}:\ u \mapsto w$ is given by

$$w[n] = \rho u[n] + \delta \left(\sum_{j=-50}^{50} u[n-j] \right)^5$$

for some (unknown) coefficients ρ and δ. One can treat $\mathbf{C}$ as a generic Volterra series expansion with fifth order monomials with delays between -50 and 50, and the first order monomial with delay 0, which leads to a basis sequence $\tilde{\mathbf{C}}$ with $1+\binom{105}{5}=96560647$ elements (and the same number of multiplications involved in implementing the compensator). Alternatively, one may realize that the two-element structure $\tilde{\mathbf{C}}=\{\mathbf{C}_1,\mathbf{C}_2\}$, with $w_k=\mathbf{C}_k u$ defined by

$$w_1[n]=u[n], \qquad w_2[n]=\left(\sum_{j=-50}^{50} u[n-j]\right)^5$$

is good enough.

In this paper we establish that a certain special structure is good enough to compensate for imperfect modulation. We consider systems represented by the block diagram

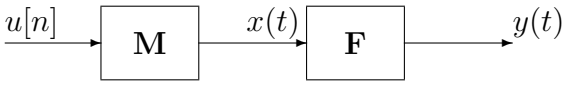

where $\mathbf{M}:\ \ell(\mathbb{C})\to\mathcal{L}(\mathbb{R})$ is the *ideal* modulator, and $\mathbf{F}:\ \mathcal{L}(\mathbb{R})\to\mathcal{L}(\mathbb{R})$ is a CT dynamical system used to represent linear and nonlinear distortion in the modulator and power amplifier circuits. We consider ideal modulator of the form $\mathbf{M}=\mathbf{XZ}$, where $\mathbf{Z}:\ \ell(\mathbb{C})\to\mathcal{L}(\mathbb{C})$ is the *zero order hold* map $u[\cdot]\mapsto x_0(\cdot)$:

$$x_0(t)=\sum_n p(t-nT)u[n], \quad p(t)=\begin{cases}1, & t\in[0,T),\\ 0, & t\notin[0,T)\end{cases}$$

with fixed sampling interval length $T>0$ and $\mathbf{X}:\ \mathcal{L}(\mathbb{C})\mapsto\mathcal{L}(\mathbb{R})$ is the *mixer* map

$$x_0(\cdot)\mapsto x(\cdot):\quad x(t)=2\mathrm{Re}[\exp(j\omega_c t)x_0(t)]$$

with modulation-to-sampling frequency ratio $M\in\mathbb{N}$, i.e., with $\omega_c=2\pi M/T$. We are particularly interested in the case when $\mathbf{F}$ is described by the *CT Volterra series model*

$$y(t)=b_0+\sum_{k=1}^{N_b} b_k\prod_{i=1}^{\beta_k} x(t-t_{k,i}), \tag{1}$$

where $N_b\in\mathbb{N}$, $b_k\in\mathbb{R}$, $\beta_k\in\mathbb{N}$, $t_{k,i}\geq 0$ are parameters. (In a similar fashion, it is possible to consider input-output relations in which the finite sum in (1) is replaced by an integral, or an infinite sum). One expects that the memory of $\mathbf{F}$ is not long, compared to T, i.e., that $\max t_{k,i}/T$ is not much larger than 1.

As a rule, the spectrum of the DT input $u\in\ell(\mathbb{C})$ of the modulator is carefully shaped at a pre-processing stage to guarantee desired characteristics of the modulated signal $x=\mathbf{M}u$. However, when the distortion $\mathbf{F}$ is not linear, the spectrum of the $y=\mathbf{F}x$ could be damaged substantially, leading to violations of EVM and spectral mask specifications [12].

Consider the possibility of repairing the spectrum of y by pre-distorting the digital input $u\in\ell(\mathbb{C})$ by a compensator $\mathbf{C}:\ \ell(\mathbb{C})\to\ell(\mathbb{C})$, as shown on the block diagram below:

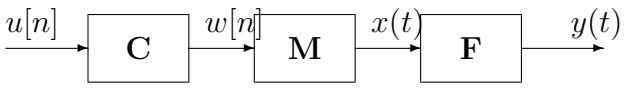

The desired effect of inserting $\mathbf{C}$ is cancellation of the distortion caused by $\mathbf{F}$. Naturally, since $\mathbf{C}$ acts in the baseband (i.e., in discrete time), there is no chance that $\mathbf{C}$ will achieve a complete correction, i.e., that the series composition $\mathbf{FMC}$ of $\mathbf{F}$, $\mathbf{M}$, and $\mathbf{C}$ will be identical to $\mathbf{M}$. However, in principle, it is sometimes possible to make the frequency contents of $\mathbf{M}u$ and $\mathbf{FMC}u$ to be identical within the CT frequency band $(\omega_c - \omega_b, \omega_c + \omega_b)$, where $\omega_b = \pi/T$ is the Nyquist frequency [18, 19]. To this end, let $\mathbf{H}: \mathcal{L}(\mathbb{R}) \to \mathcal{L}(\mathbb{R})$ denote the ideal band-pass filter with frequency response

$$H(\omega) = \begin{cases} 1, & |\,\omega_c - |\omega|\,| < \omega_b, \\ 0, & \text{otherwise.} \end{cases} \tag{2}$$

Let $\mathbf{D}: \mathcal{L}(\mathbb{R}) \to \ell(\mathbb{C})$ be the *ideal de-modulator* relying on the band selected by $\mathbf{H}$, i.e. the linear system for which the series composition $\mathbf{DHM}$ is the identity function. Let $\mathbf{S} = \mathbf{DHFM}$ be the series composition of $\mathbf{D}$, $\mathbf{H}$, $\mathbf{F}$, and $\mathbf{M}$, i.e. the DT system with input $w = w[n]$ and output $v = v[n]$ shown on the block diagram below:

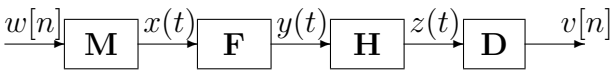

Figure 1: Block diagram of $\mathbf{S} = \mathbf{DHFM}$

By construction, the ideal compensator $\mathbf{C}$ should be the inverse $\mathbf{C} = \mathbf{S}^{-1}$ of $\mathbf{S}$, as long as the inverse does exist.

A key question answered in this paper is "what to expect from system $\mathbf{S}$?" If one assumes that the continuous-time distortion subsystem $\mathbf{F}$ is simple enough, what does this say about $\mathbf{S}$?

This paper provides an explicit expression for $\mathbf{S}$ in the case when $\mathbf{F}$ is given in the CT Volterra series form (1) with *degree* $d = \max \beta_k$ and *depth* $t_{max} = \max t_{k,i}$. The result reveals that, even though $\mathbf{S}$ tends to have infinitely long memory (due to the ideal band-pass filter $\mathbf{H}$ being involved in the construction of $\mathbf{S}$), it can be represented as a series composition $\mathbf{S} = \mathbf{LV}$, where $\mathbf{V}: \ell(\mathbb{C}) \to \ell(\mathbb{R}^N)$ maps scalar complex input $w \in \ell(\mathbb{C})$ to real vector output $g \in \ell(\mathbb{R}^N)$ in such a way that the k-th scalar component $g_k[n]$ of $g[n] \in \mathbb{R}^N$ is given by

$$g_k[n] = \prod_{i=0}^{m} (\text{Re}\; w[n-i])^{\alpha_i} \prod_{i=0}^{m} (\text{Im}\; w[n-i])^{\beta_i}, \qquad \alpha_i, \beta_i \in \mathbb{Z}_+, \qquad \sum_{i=0}^{m} \alpha_i + \sum_{i=0}^{m} \beta_i \le d,$$

m is the minimal integer not smaller than t_{max}/T, and $\mathbf{L}: \ell(\mathbb{R}^N) \to \ell(\mathbb{C})$ is an LTI system. Moreover, $\mathbf{L}$ can be shown to have a good approximation of the form $\mathbf{L} \approx X\mathbf{L}_0$, where X is a static gain matrix, and $\mathbf{L}_0$ is an LTI model which does not depend on b_k and $t_{k,i}$. In other words, $\mathbf{S}$ can be well approximated by combining a Volterra series model with a short memory,

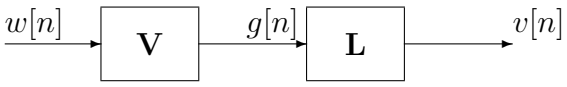

Figure 2: Block diagram of the structure of $\mathbf{S}$

and a *fixed* (long memory) LTI, as long as the memory depth t_{max} of $\mathbf{F}$ is short, relative to the sampling time T.

In most applications, with an appropriate scaling and time delay, the system $\mathbf{S}$ to be inverted can be viewed as a small perturbation of identity, i.e. $\mathbf{S} = \mathbf{I} + \mathbf{\Delta}$. When $\mathbf{\Delta}$ is "small" in an appropriate sense (e.g., has small incremental L2 gain $\|\mathbf{\Delta}\| \ll 1$), the inverse of $\mathbf{S}$ can be well approximated by $\mathbf{S}^{-1} \approx \mathbf{I} - \mathbf{\Delta} = 2\mathbf{I} - \mathbf{S}$. Hence the result of this paper suggests a specific structure of the compensator (pre-distorter) $\mathbf{C} \approx \mathbf{I} - \mathbf{\Delta} = 2\mathbf{I} - \mathbf{S}$. In other words, a plain Volterra monomials structure is, in general, not good enough for $\mathbf{C}$, as it lacks the capacity to implement the long-memory LTI post-filter $\mathbf{L}$. Instead, $\mathbf{C}$ should be sought in the form $\mathbf{C} = \mathbf{I} - \mathbf{L_0} X \mathbf{V}$, where $\mathbf{V}$ is the system generating all Volterra series monomials of a limited depth and limited degree, $\mathbf{L}_0$ is a *fixed* LTI system with a very long time constant, and X is a matrix of coefficients to be optimized to fit the data available.

3.1 Ideal Demodulator

The most commonly known expression for the ideal demodulator inverts not $\mathbf{M} = \mathbf{XZ}$ but $\mathbf{M}_0 = \mathbf{XH}_0\mathbf{Z}$, i.e., the modulator which inserts $\mathbf{H}_0$, the *ideal low-pass filter* for the baseband, between zero-order hold $\mathbf{Z}$ and mixer $\mathbf{X}$, where $\mathbf{H}_0$ is the CT LTI system with frequency response

$$H_0(\omega) = \begin{cases} 1, & |\omega| < \omega_b, \\ 0, & \text{otherwise.} \end{cases}$$

Specifically, let $\mathbf{X}_c : \mathcal{L}(\mathbb{R}) \mapsto \mathcal{L}(\mathbb{C})$ be the *dual mixer* mapping $x(\cdot)$ to $e(t) = \exp(-j\omega_c t)x(t)$. Let $\mathbf{E} : \mathcal{L}(\mathbb{C}) \mapsto \ell(\mathbb{C})$ be the *sampler*, mapping $g(\cdot)$ to $w[n] = g(nT)$. Finally, let $\mathbf{A}_0$ be the DT LTI system with frequency response A_0 defined by

$$A_0(\Omega) = P(\Omega/T)^{-1} \quad \text{for} \quad |\Omega| < \pi,$$

where P is the Fourier transform of $p = p(t)$. Then the composition $\mathbf{A}_0\mathbf{E}\mathbf{H}_0\mathbf{X}_c\mathbf{H}\mathbf{M}_0$ is an identity map. Equivalently, $\mathbf{A}_0\mathbf{E}\mathbf{H}_0\mathbf{X}_c$ is the ideal demodulator for $\mathbf{M}_0$.

For the modulation map $\mathbf{M} = \mathbf{XZ}$ considered in this paper, the ideal demodulator has the form $\mathbf{AEH}_0\mathbf{X}_c$, where $\mathbf{A} : \ell(\mathbb{C}) \mapsto \ell(\mathbb{C})$ is the linear system mapping $w \in \ell(\mathbb{C})$ to $s \in \ell(\mathbb{C})$ according to

$$\text{Re}(s) = \mathbf{A}_{rr}\text{Re}(w) + \mathbf{A}_{ri}\text{Im}(w),$$
$$\text{Im}(s) = \mathbf{A}_{ir}\text{Re}(w) + \mathbf{A}_{ii}\text{Im}(w),$$

and $\mathbf{A}_{rr}$, $\mathbf{A}_{ri}$, $\mathbf{A}_{ir}$, $\mathbf{A}_{ii}$ are LTI systems with frequency responses $A_{rr} = (P_0 - P_i)Q$, $A_{ir} = A_{ri} = -P_qQ$, $A_{ii} = (P_0 + P_i)Q$, where $Q = (P_0^2 - P_i^2 - P_q^2)^{-1}$, $P_i = (P^+ + P^-)/2$,

$P_q = (P^+ - P^-)/2j$, and $P_0, P^+, P^- \in \mathcal{L}[\mathbb{C}]$ are defined for $|\Omega| < \pi$ by

$$P_0(\Omega) = P(\Omega/T),\ P^+(\Omega) = P_0(\Omega + \theta),\ P^-(\Omega) = P_0(\Omega - \theta)$$

with $\theta = 4\pi M$.

Proof. For signals u, $u_i = \mathrm{Re}(u)$, $u_q = \mathrm{Im}(u)$, $w = \mathbf{EH_0X_cHM_0}u$, $w_i = \mathrm{Re}(w)$, $w_q = \mathrm{Im}(w)$, and their Fourier transforms U, U_i, U_q, W, W_i, W_q we have $U = U_i + jU_q$, $W = W_i + jW_q$, and

$$W(\Omega) = P_0(\Omega)U(\Omega) + \tilde{P}(\Omega)\overline{U(-\Omega)},$$

where $\tilde{P}(\Omega) = P(\Omega/T + 2\omega_c))$, i.e., $\tilde{P} = P_i + jP_q$. Hence U_i, U_q satisfy the equations

$$(P_0 + P_i)U_i + P_qU_q = W_i,\ P_qU_i + (P_0 - P_i)U_q = W_q,$$

which can be used to express U_i, U_q in terms of W_i, W_q. □

4 Main Result

Before stating our main theorem, we will introduce some additional notation.
Let d be a given positive integer, and $\tau = (\tau_1, \ldots, \tau_d)$ be a d-tuple of non-negative real numbers τ_i. Let $\mathbf{F}_\tau :\ \mathcal{L} \to \mathcal{L}$ be the CT system mapping inputs $x \in \mathcal{L}$ to the outputs $y \in \mathcal{L}$ defined by

$$y(t) = x(t - \tau_1)x(t - \tau_2)\ldots x(t - \tau_d).$$

For each d-tuple $\mathbf{m} = (m_1, \ldots, m_d) \in [4]^d$ and integer $l \in [4]$ we define set S_m^l to be the set of all indices i for which $m_i = l$, i.e. $S_m^l = \{i \in [d] :\ m_i = l\}$. We further define

$$N_m^1 = |S_m^1 \cup S_m^2|,\ N_m^2 = |S_m^3 \cup S_m^4|.$$

Clearly $N_m^1 + N_m^2 = d$ for each $m \in [4]^d$. Let $R_m^c = \{-1, 1\}^{N_m^1}$ and $R_m^s = \{-1, 1\}^{N_m^2}$.

Let $(\cdot, \cdot) : \mathbb{R}^d \times \mathbb{R}^d \to \mathbb{R}$ be the standard scalar product in $\mathbb{R}^d$, and let maps $\tilde{\sigma}, \sigma : \mathbb{R}^d \to \mathbb{R}$ be defined by $\tilde{\sigma}(x) = \sum_{i=1}^d x_i$ and $\sigma(x) = \tilde{\sigma}(x) - 1$. For a given $m \in [4]^d$ and $x \in \mathbb{R}^d$ let $\pi_m(x)$ be the product of all x_i with $i \in S_m^3 \cup S_m^4$. For $i \in \{1, 2\}$ we define projection operators $\mathcal{P}_m^i : \mathbb{R}^d \to \mathbb{R}^{N_m^i}$ by

$$\mathcal{P}_m^i x = \begin{bmatrix} x_{n_1} & \ldots & x_{n_{N_m^i}} \end{bmatrix}^T, \quad \{n_1, \ldots, n_{N_m^i}\} = S_m^{2i-1} \cup S_m^{2i}, \quad n_1 < \cdots < n_{N_m^i}.$$

Given a vector $\tau \in \mathbb{R}_+^d$ let $\mathbf{k}$ be a vector in $(\mathbb{N} \cup \{0\})^d$, such that $\tau = \mathbf{k}T + \tau'$, with $\tau' \in [0, T)^d$. It is obvious that for a given τ vector $\mathbf{k}$ is uniquely defined.

Given a positive real number T, let us denote by $p(t)$, the basic pulse shape of the zero-order hold (ZOH) system. We have $p(t) = \theta(t) - \theta(t - T)$, where θ is the Heaviside step function. Moreover for a given $m \in [4]^d$ and $\tau' \in [0, T)^d$,we define

$$\tau_{min}^m = \begin{cases} \max_{i \in S_m^2 \cup S_m^4} \tau_i', & |S_m^2 \cup S_m^4| > 0 \\ 0, & o/w \end{cases},$$

and

$$\tau_{max}^m = \begin{cases} \min_{i \in S_m^1 \cup S_m^3} \tau_i', & |S_m^1 \cup S_m^3| > 0 \\ T, & o/w \end{cases}.$$

Now let $p_{m,\tau} : \mathbb{R} \to \mathbb{R}$ be the continuous time signal defined by

$$p_{m,\tau}(t) = \begin{cases} \theta(t - \tau_{min}^m) - \theta(t - \tau_{max}^m), & \tau_{min}^m < \tau_{max}^m \\ 0, & o/w \end{cases}. \tag{3}$$

We denote its Fourier transform by $P_{m,\tau}(\omega)$.

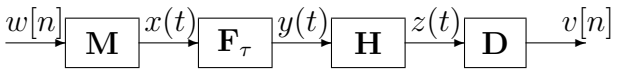

Figure 3: Block diagram of system $\mathbf{S}_\tau = \mathbf{DHF}_\tau\mathbf{M}$

From expression (1), describing CT Volterra series, we can see that the general CT Volterra model is a linear combination of subsystems of form $\mathbf{F}_\tau$. Thus in order to find system decomposition $\mathbf{S} = \mathbf{LV}$ it is clearly sufficient to find what happens with one particular element $\mathbf{F}_\tau$, i.e. to find map $\mathbf{S}_\tau = \mathbf{DHF}_\tau\mathbf{M}$ (block diagram depicted in Fig. 3). The following theorem gives an answer to that question.

Theorem 4.1. A DT system $\mathbf{DHF}_\tau\mathbf{M} : \ell(\mathbb{C}) \to \ell(\mathbb{C})$, mapping $w[n] = i[n] + j \cdot q[n]$ to $v[n]$, is given by

$$v[n] = (\mathbf{A}u)[n],$$

where

$$u = \sum_{m \in [4]^d} x_{m,k} * g_m,$$

$$x_{m,k}[n] = \prod_{i \in S_m^1} i[n - k_i - 1] \cdot \prod_{i \in S_m^2} i[n - k_i] \cdot \prod_{i \in S_m^3} q[n - k_i - 1] \cdot \prod_{i \in S_m^4} q[n - k_i],$$

and Fourier transform of a unit sample response $g_m[n]$ is given by

$$G_m(\Omega) = \frac{(j)^{N_m^2}}{2^d} \sum_{r_c \in R_m^c} \sum_{r_s \in R_m^s} \prod_{l=1}^{N_m^2} r_c(l) \cdot P_{m,\tau}\left(\frac{\Omega}{T} - \omega_c \sum_i r_c(i) - \omega_c \sum_l r_s(l) + \omega_c\right) \cdot e^{-j\omega_c[(r_c, \mathcal{P}_m^1 \tau) + (r_s, \mathcal{P}_m^2 \tau)]}.$$

Proof. We first state and prove the following Lemma, which is very similar to Theorem 4.1 but considers somewhat simpler case when $\tau \in [0, T)^d$, i.e. $\mathbf{k} = \mathbf{0}$. The proof of Theorem 4.1 then immediately follows from this Lemma.

Lemma 4.2. Suppose that $\tau \in [0,T)^d$. A DT system $\mathbf{DHF}_\tau\mathbf{M} : \ell(\mathbb{C}) \to \ell(\mathbb{C})$, mapping $w[n] = i[n] + j \cdot q[n]$ to $v[n]$, is given by

$$v[n] = (\mathbf{A}u)[n],$$

where

$$u = \sum_{m\in[4]^d} x_m * g_{m,\tau},$$

$$x_m[n] = i[n-1]^{|S_m^1|} \cdot i[n]^{|S_m^2|} \cdot q[n-1]^{|S_m^3|} \cdot q[n]^{|S_m^4|},$$

and Fourier transform of a unit sample response $g_{m,\tau}[n]$ is given by

$$G_{m,\tau}(\Omega) = \frac{(j)^{N_m^2}}{2^d} \sum_{r_c\in R_m^c} \sum_{r_s\in R_m^s} \prod_{l=1}^{N_m^2} r_c(l)\cdot P_{m,\tau}\left(\frac{\Omega}{T} - \omega_c \sum_i r_c(i) - \omega_c \sum_l r_s(l) + \omega_c\right)\cdot e^{-j\omega_c[(r_c,\mathcal{P}_m^1\tau)+(r_s,\mathcal{P}_m^2\tau)]}.$$

Proof. Let us first analyze what happens in the case when $d = 1$, i.e. when system $\mathbf{F}_\tau$ is just a delay by $\tau \in [0,T)$. Detailed block diagram of system $\mathbf{DHF}_\tau\mathbf{M}$ is depicted in Fig. 4, where $\mathbf{M}$ and $\mathbf{D}$ are decomposed into elementary subsystems as defined in the previous chapter.

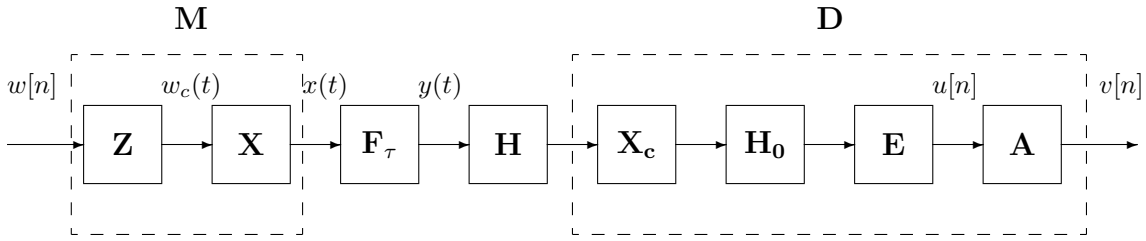

Figure 4: Block diagram of system $\mathbf{S}_\tau = \mathbf{DHF}_\tau\mathbf{M}$

Output $w_c(t)$ of $\mathbf{Z}$ is given by

$$w_c(t) = \frac{1}{T}\sum_{n=-\infty}^{\infty} w[n]p(t-nT) = \underbrace{\frac{1}{T}\sum_{n=-\infty}^{\infty} i[n]p(t-nT)}_{i_c(t)} + \underbrace{\frac{j}{T}\sum_{n=-\infty}^{\infty} w[n]p(t-nT)}_{jq_c(t)}.$$

It follows that

$$x(t) = (\mathbf{X}w_c)(t) = \mathrm{Re}\{\exp(j\omega_c t)w_c(t)\},$$

and output $y(t)$ of $\mathbf{F}_\tau$ becomes

$$y(t) = i_c(t-\tau)\cos(\omega_c t - \omega_c\tau) - q_c(t-\tau)\sin(\omega_c t - \omega_c\tau).$$

Let us decompose $p(t)$ as $p(t) = p_{1,\tau}(t) + p_{2,\tau}(t)$, where

$$p_{1,\tau}(t) = \theta(t) - \theta(t-\tau),$$

$$p_{2,\tau}(t) = \theta(t-\tau) - \theta(t-T).$$

Let $\mathbf{Z_1} : \ell(\mathbb{C}) \to \mathcal{L}(\mathbb{C})$ and $\mathbf{Z_2} : \ell(\mathbb{C}) \to \mathcal{L}(\mathbb{C})$ be digital-to-analog converters with pulse shapes given by signals $p_{1,\tau}$ and $p_{2,\tau}$ respectively. It can be seen that signals $i_c(t-\tau)$ and $q_c(t-\tau)$ can be decomposed as

$$i_c(t-\tau) = (\mathbf{Z_1}(z^{-1}i))(t) + (\mathbf{Z_2}i)(t),$$

$$q_c(t-\tau) = (\mathbf{Z_1}(z^{-1}q))(t) + (\mathbf{Z_2}q)(t),$$

where $z^{-1} : x[n] \mapsto x[n-1]$ is the backshift map. Let us denote componenets of $i_c(t-\tau)$ and $q_c(t-\tau)$ as

$$e_{1,\tau}(t) = (\mathbf{Z_1}(z^{-1}i))(t), \qquad e_{2,\tau}(t) = (\mathbf{Z_2}i)(t),$$
$$e_{3,\tau}(t) = (\mathbf{Z_1}(z^{-1}q))(t), \qquad e_{4,\tau}(t) = (\mathbf{Z_2}q)(t).$$

Thus signals $e_{j,\tau}(t)$, $j \in [4]$, are obtained by applying digital-to-analog converters $\mathbf{Z_1}$ and $\mathbf{Z_1}$ on in-phase or quadrature components of the input signal $w[n]$ (or their delayed counterparts). It follows that signals $e_{i,\tau}(t)$ can be written as

$$\begin{aligned}
e_{1,\tau}(t) &= \frac{1}{T}\sum_{n=-\infty}^{\infty} i[n-1]p_{1,\tau}(t-nT),\\
e_{2,\tau}(t) &= \frac{1}{T}\sum_{n=-\infty}^{\infty} i[n]p_{2,\tau}(t-nT),\\
e_{3,\tau}(t) &= -\frac{1}{T}\sum_{n=-\infty}^{\infty} q[n-1]p_{1,\tau}(t-nT),\\
e_{4,\tau}(t) &= -\frac{1}{T}\sum_{n=-\infty}^{\infty} q[n]p_{2,\tau}(t-nT).
\end{aligned} \tag{4}$$

It follows that $\mathbf{F}_\tau$ in some sense commutes with the modulation subsystem $\mathbf{M}$, following an appropriate decomposition of the ZOH pulse function, thus allowing us to move $\mathbf{F}_\tau$ out of the passband part of the system.

Now system $\mathbf{DHF}_\tau\mathbf{M}$ can be represented by the block diagram shown in Fig. 5, where $\tilde{\mathbf{D}}$ denotes the composition $\mathbf{EH_0X_cH}$.

Thus subsystem $\mathbf{F}_\tau\mathbf{M}$, mapping $w[n]$ to $y(t)$, can be represented as a parallel connection of four LTI systems whose inputs are current and previous values of in-phase and quadrature components of the input signal $w[n]$.

If we define signals $f_i(t)$ as

$$f_i(t) = \begin{cases} e_{i,\tau}(t)\cos(\omega_c t - \omega_c\tau), & i = 1,2\\ e_{i,\tau}(t)\sin(\omega_c t - \omega_c\tau), & i = 3,4 \end{cases} \tag{5}$$

output $y(t)$ of $\mathbf{F}_\tau$ can be written as:

$$y(t) = f_1(t) + f_2(t) + f_3(t) + f_4(t).$$

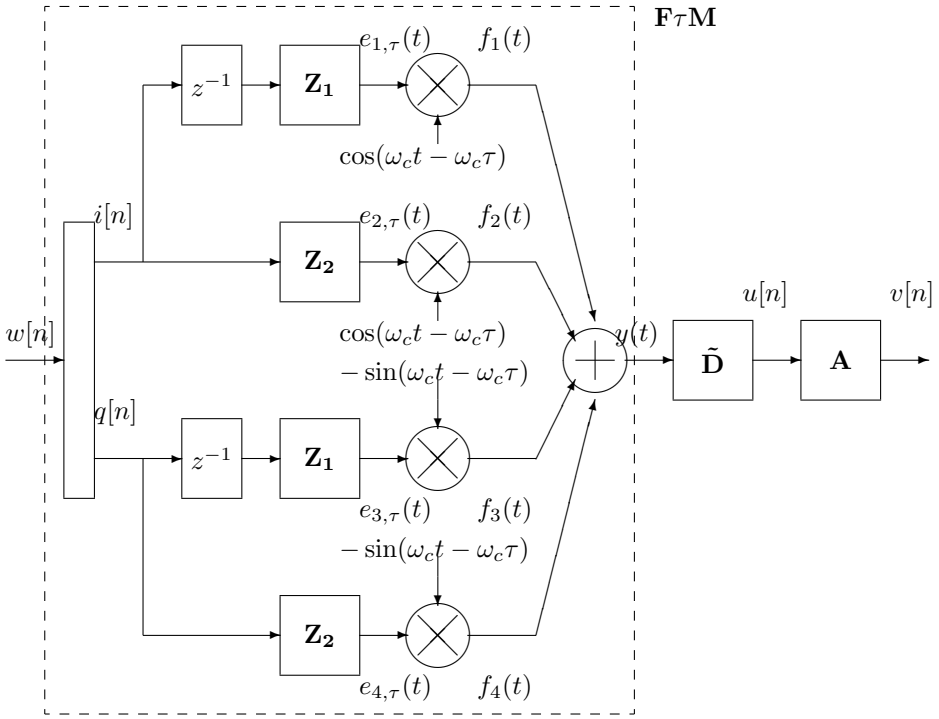

Figure 5: Equivalent representation of $\mathbf{DHF}_\tau\mathbf{M}$

Now suppose that order d of $\mathbf{F}_\tau$ is an arbitrary positive integer larger than 1, i.e. that $\mathbf{F}_\tau : x \mapsto x(t-\tau_1) \cdot \dots \cdot x(t-\tau_d)$. Now output $y(t)$ of $\mathbf{F}_\tau$ can be written as

$$\begin{aligned} y(t) = [i_c(t-\tau_1)\cos(\omega_c t - \omega_c\tau_1) - q_c(t-\tau_1)\sin(\omega_c t - \omega_c\tau_1)]\cdot \\ \cdot [i_c(t-\tau_2)\cos(\omega_c t - \omega_c\tau_2) - q_c(t-\tau_2)\sin(\omega_c t - \omega_c\tau_2)]\cdot \dots \\ \dots \cdot [i_c(t-\tau_d)\cos(\omega_c t - \omega_c\tau_d) - q_c(t-\tau_d)\sin(\omega_c t - \omega_c\tau_d)]. \end{aligned} \quad (6)$$

Let us denote the factors in product in (6) as $y_i(t)$, i.e.

$$y_i(t) = i_c(t-\tau_i)\cos(\omega_c t - \omega_c\tau_i) - q_c(t-\tau_i)\sin(\omega_c t - \omega_c\tau_i).$$

It is clear that for each i, signal $y_i(t)$ can be represented as the output of subsystem $\mathbf{F}_{\tau_i}\mathbf{M}$. Thus subsystem $\mathbf{F}_\tau\mathbf{M}$ can be represented as a parallel connection of d subsystems $\mathbf{F}_{\tau_i}\mathbf{M}$, with outputs $y_i(t)$, where output $y(t)$ of $\mathbf{F}_\tau\mathbf{M}$ is equal to $y(t) = y_1(t) \cdot \dots \cdot y_d(t)$. This is depicted in Fig. 6. Hence, by using the same notation as in Figs 5 and 6, signal $y(t)$ can be written as

$$y(t) = \prod_{i=1}^{d} y_i(t) = \prod_{i=1}^{d} (f_1^i(t) + f_2^i(t) + f_3^i(t) + f_4^i(t)) = \sum_{m\in[4]^d} f_{m_1}^1(t) \cdot \dots \cdot f_{m_d}^d(t). \quad (7)$$

Let us denote product $f_{m_1}^1(t) \cdot \dots \cdot f_{m_d}^d(t)$ with $f_m(t)$. Now $y(t)$ can be written as

$$y(t) = \sum_{m\in[4]^d} f_m(t). \quad (8)$$

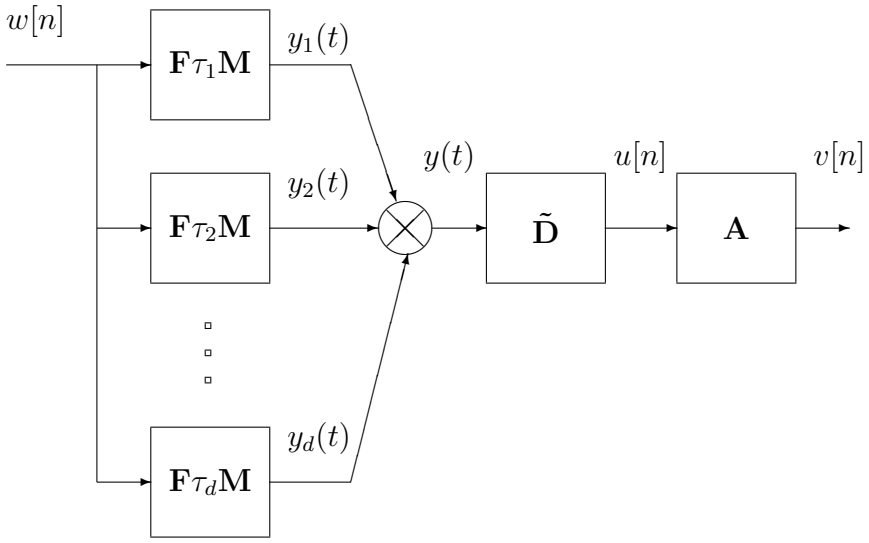

Figure 6:

Here componenets m_i of $m = (m_1,\ m_2,\ \ldots,\ m_d) \in [4]^d$, determine which signal f_j^i, $j \in [4]$ from (5) participates as a product factor in $f_m(t)$. With signals $e_{m_i,\tau_i}(t)$ as defined in (18), it is clear that summands in (8) can be written as

$$f_m(t) = (-1)^{N_m^2} \prod_{i=1}^{d} e_{m_i,\tau_i}(t) \cdot \prod_{k \in S_m^1 \cup S_m^2} \cos(\omega_c t - \omega_c \tau_k) \cdot \prod_{l \in S_m^3 \cup S_m^4} \sin(\omega_c t - \omega_c \tau_l). \quad (9)$$

Since our goal is to find transfer functions from $x_m[n]$ to $v[n]$, it is more convenient to express the above products of cosines and sines as sums of complex exponentials, i.e.

$$\prod_{k \in S_m^1 \cup S_m^2} \cos(\omega_c t - \omega_c \tau_k) = \frac{1}{2^{N_m^1}} \sum_{r \in R_m^c} e^{j\omega_c \bar{\sigma}(r) t} \cdot e^{-j\omega_c (r, \mathcal{P}_m^1 \tau)}, \quad (10)$$

$$\prod_{l \in S_m^3 \cup S_m^4} \sin(\omega_c t - \omega_c \tau_l) = \frac{1}{(2j)^{N_m^2}} \sum_{r \in R_m^s} \prod_{i=1}^{N_m^2} r(i) \cdot e^{j\omega_c \bar{\sigma}(r) t} \cdot e^{-j\omega_c (r, \mathcal{P}_m^2 \tau)}. \quad (11)$$

As emphasized earlier, signals $e_{m_i,\tau_i}(t)$ are obtained by applying pulse amplitude modulation with $p_{1,\tau_i}(t)$ or $p_{2,\tau_i}(t)$ on in-phase or quadrature components of the input signal (or their delayed counterparts). Let us denote the product of signals $e_{m_i,\tau_i}(t)$ in (9) as $e_{m,\tau}(t)$. We want to find an expression for $e_{m,\tau}(t)$ as a function of signals $i[n], (z^{-1}i)[n], q[n]$, and $(z^{-1}q)[n]$. Let us first investigate signal $e_{m,\tau}(t)$ for $t \in [nT, (n+1)T)$, with $n > 1$ an integer. There are three possible cases:

(i) $S_m^2 \cup S_m^4 = \emptyset$, i.e. signals $e_{m_i,\tau_i}(t)$ were all obtained by applying pulse amplitude modulation with $p_{1,\tau}(t)$. It immediately follows that product $e_{m,\tau}(t)$ of signals $e_{m_i,\tau_i}(t)$ is nonzero only for $t \in [nT, nT + \tau_{max})$, where $\tau_{max} = \min_i \tau_i$.

(ii) $S_m^1 \cup S_m^3 = \emptyset$, i.e. signals $e_{m_i,\tau_i}(t)$ were all obtained by applying pulse amplitude modulation with $p_{2,\tau}(t)$. It immediately follows that product $e_{m,\tau}(t)$ of signals $e_{m_i,\tau_i}(t)$ is nonzero only for $t \in [nT + \tau_{min}, (n+1)T)$, where $\tau_{min} = \max_i \tau_i$.

(iii) Both $S_m^1 \cup S_m^3$ and $S_m^2 \cup S_m^4$ are non-empty. Let $\tau_{min} = \max_{i \in S_m^2 \cup S_m^4} \tau_i$ and $\tau_{max} = \min_{i \in S_m^1 \cup S_m^3} \tau_i$. It then follows from the previous two cases that if $\tau_{min} > \tau_{max}$, product $e_{m,\tau}(t)$ is equal to zero for all $t \in [nT, (n+1)T)$. Otherwise it is nonzero for $t \in [nT + \tau_{min}, nT + \tau_{max})$. This is depicted in Fig. 7 (for the sake of simplicity, only in-phase component i is considered, but in general signals $q[n]$ and $q[n-1]$ would appear too).

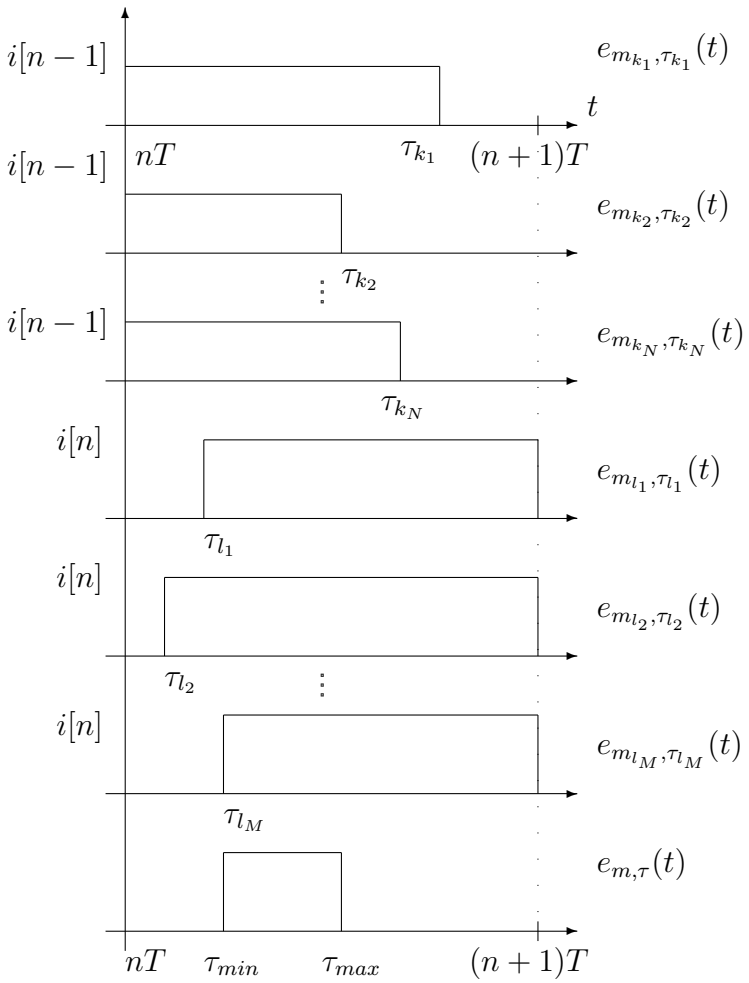

Figure 7: Signal $e_{m,\tau}$ for $S_m^1 \cup S_m^3 = \{k_1, k_2, \ldots, k_N\}$ and $S_m^2 \cup S_m^4 = \{l_1, l_2, \ldots, l_M\}$, where $N + M = d$

Now it directly follows that $e_{m,\tau}(t)$ can be written as

$$e_{m,\tau}(t) = \sum_{n=-\infty}^{\infty} i[n]^{|S_m^1|} \cdot i[n-1]^{|S_m^2|} \cdot q[n]^{|S_m^3|} \cdot q[n-1]^{|S_m^4|} p_{m,\tau}(t-nT), \tag{12}$$

where $p_{m,\tau}(t)$ was defined in (3). Let us denote DT signal in (12) as $x_m[n]$, i.e.

$$x_m[n] = i[n]^{|S_m^1|} \cdot i[n-1]^{|S_m^2|} \cdot q[n]^{|S_m^3|} \cdot q[n-1]^{|S_m^4|}.$$

Now from (12), (10) and (11), it follows that signal $f_m(t)$, can be written as

$$f_m(t) = f_{m_1}^1(t) \cdot \ldots \cdot f_{m_d}^d(t) = \sum_{n=-\infty}^{\infty} x_m[n] p_{m,\tau}(t-nT) \cdot \sum_{r_c \in R_m^c} \sum_{r_s \in R_m^s} C_{r_c,r_s} \cdot e^{j\sigma(r_c,r_s)\omega_c t}, \tag{13}$$

where $\sigma(r_c, r_s) = \sum_k r_c(k) + \sum_l r_s(l)$, and

$$C_{r_c,r_s} = \frac{(j)^{N_m^2}}{2^d} \cdot e^{-j\omega_c[(r_c,\mathcal{P}_m^1\tau)+(r_s,\mathcal{P}_m^2\tau)]} \cdot \prod_{k=1}^{N_m^2} r_s(k), \tag{14}$$

depend only on m. In the rest of this proof, for a given r_c and r_s we will denote $\sigma(r_c, r_s)$ with $\sigma(r)$.
Hence signal y(t), which is given in (8), is a sum of scaled and modulated copies of signal $e_{m,\tau}(t)$. This gives us an explicit dependence relation between $y(t)$ and signals $x_m[n]$.

In order to find a transfer function from $x_m[n]$ to $u[n]$, let us first find relation, in fequency domain, between signals $y(t)$ and $u[n]$. Recall that $u = \tilde{\mathbf{D}}y = \mathbf{E}\mathbf{H_0}\mathbf{X_c}\mathbf{H}y$. Let us denote the Fourier transforms of signals $u[n]$ and $y(t)$ with $U(\Omega)$ and $Y(\omega)$ respectively. Also let $H(\omega)$ and $H_0(\omega)$ be the frequency responses of ideal band-pass and low-pass filters $\mathbf{H}$ and $\mathbf{H_0}$, given by

$$\begin{aligned} H(\omega) &= \begin{cases} 1, & \omega_c - \pi/T \le |\omega| \le \omega_c + \pi/T \\ 0, & \text{o/w} \end{cases}, \\ H_0(\omega) &= \begin{cases} 1, & |\omega| \le \pi/T \\ 0, & \text{o/w} \end{cases}. \end{aligned} \tag{15}$$

Now we have the following sequence of equalities

$$\begin{aligned} \mathcal{F}\{\mathbf{H}y\} &= Y(\omega)H(\omega), \\ \mathcal{F}\{\mathbf{X_c}\mathbf{H}y\} &= Y(\omega+\omega_c)H(\omega+\omega_c), \\ \mathcal{F}\{\mathbf{H_0}\mathbf{X_c}\mathbf{H}y\} &= Y(\omega+\omega_c)H(\omega+\omega_c)H_o(\omega), \\ U(\Omega) &= Y\left(\frac{\Omega}{T}+\omega_c\right) H\left(\frac{\Omega}{T}+\omega_c\right) H_0\left(\frac{\Omega}{T}\right). \end{aligned}$$

Due to definition of $H(\omega)$ and $H_0(\omega)$, $U(\Omega)$ simplifies to

$$U(\Omega) = Y\left(\frac{\Omega}{T} + \omega_c\right). \tag{16}$$

Next we express $Y(\omega)$ in terms of $X_m(\Omega) = \mathcal{F}\{x_m[n]\}$. For the sake of simplicity, we assume that $y(t) = f_m(t)$ for some fixed m, i.e. we omit the sum in (8). From (13) it follows that

$$\mathcal{F}\{f_m(t)\} = Y(\omega) = \sum_{r_c \in R_m^c} \sum_{r_s \in R_m^s} C_{r_c,r_s} X_m\left(\omega T - \sigma(r)\cdot\omega_c T\right) P_{m,\tau}\left(\omega - \sigma(r)\cdot\omega_c\right).$$

Since $\omega_c T = 2\pi n$, where $n \in \mathbb{Z}$, we get

$$Y(\omega) = X_m(\omega T)\cdot \sum_{r_c \in R_m^c} \sum_{r_s \in R_m^s} C_{r_c,r_s} P_{m,\tau}\left(\omega - \sigma(r)\cdot\omega_c\right). \tag{17}$$

It follows from (16) and (17) that

$$U(\Omega) = X_m(\Omega)\cdot \sum_{r_c} \sum_{r_s} C_{r_c,r_s} P_{m,\tau}\left(\frac{\Omega}{T} - \omega_c\cdot\sigma(r) + \omega_c\right).$$

Therefore the frequency response from $x_m[n]$ to $u[n]$ is given by

$$G_m(\Omega) = \sum_{r_c \in R_m^c} \sum_{r_s \in R_m^s} C_{r_c,r_s} P_{m,\tau}\left(\frac{\Omega}{T} - \omega_c\cdot\sigma(r) + \omega_c\right).$$

Finally it follows that the output $v[n]$ of system $\mathbf{S}_\tau$ is equal to

$$v[n] = (\mathbf{A}u)[n],$$

where

$$u = \sum_{m\in[4]^d} x_m * g_m,$$

$$x_m[n] = i[n-1]^{|S_m^1|}\cdot i[n]^{|S_m^2|}\cdot q[n-1]^{|S_m^3|}\cdot q[n]^{|S_m^4|},$$

and frequency responses $G_m(\Omega) = \mathcal{F}\{g_m[n]\}$ are given by

$$G_m(\Omega) = \sum_{r_c \in R_m^c} \sum_{r_s \in R_m^s} C_{r_c,r_s} P_{m,\tau}\left(\frac{\Omega}{T} - \omega_c\cdot\sigma(r) + \omega_c\right),$$

with C_{r_c,r_s} as given in (14).
This concludes the proof of Lemma 4.2. □

In Lemma 4.2 we assumed that $\tau_i \in [0, T),\ \forall i \in [d]$, but in general τ_i can take any positive real value depending on the depth of (2), i.e. vector $\mathbf{k}$ associated to τ is not necessarily the zero vector. Now assume that $\tau = \mathbf{k}T + \bar{\tau}$, where $\bar{\tau} \in [0, T)^d$, and $\mathbf{k} \neq \mathbf{0}$. In the rest of this proof we assume the same notation for signals and systems as in the proof of Lemma 4.2.
Let us again first look at the case of $d = 1$, i.e. $\tau = kT + \bar{\tau}$, with $k \in \mathbb{N}$ and $\bar{\tau} \in [0, T)$. As in the proof of Lemma 2.2, we have that the output $y(t)$ of $\mathbf{F}_\tau$ becomes

$$y(t) = i_c(t - \tau)\cos(\omega_c t - \omega_c \tau) - q_c(t - \tau)\sin(\omega_c t - \omega_c \tau).$$

Now we decompose $p(t)$ as $p(t) = p_{1,\tau}(t) + p_{2,\tau}(t)$, where

$$p_{1,\tau}(t) = \theta(t) - \theta(t - \bar{\tau}),$$

$$p_{2,\tau}(t) = \theta(t - \bar{\tau}) - \theta(t - T).$$

It follows that signals $i_c(t - \tau)$ and $q_c(t - \tau)$ can be decomposed as

$$i_c(t - \tau) = (\mathbf{Z_1}(z^{-k-1}i))(t) + (\mathbf{Z_2}(z^{-k}i))(t),$$

$$q_c(t - \tau) = (\mathbf{Z_1}(z^{-k-1}q))(t) + (\mathbf{Z_2}(z^{-k}q))(t),$$

where $z^{-k} : x[n] \mapsto x[n - k]$ is the k-times backshift map. Let us denote componenets of $i_c(t - \tau)$ and $q_c(t - \tau)$ as

$$e_{1,\tau}(t) = (\mathbf{Z_1}(z^{-k-1}i))(t), \qquad e_{2,\tau}(t) = (\mathbf{Z_2}(z^{-k}i))(t),$$

$$e_{3,\tau}(t) = (\mathbf{Z_1}(z^{-k-1}q))(t), \qquad e_{4,\tau}(t) = (\mathbf{Z_2}(z^{-k}q))(t).$$

Thus signals $e_{j,\tau}(t)$, $j \in [4]$, are obtained by applying digital-to-analog converters $\mathbf{Z_1}$ and $\mathbf{Z_1}$ on delayed in-phase or quadrature components of the input signal $w[n]$. It follows that signals $e_{j,\tau}(t)$ can be written as

$$\begin{aligned}
e_{1,\tau}(t) &= \frac{1}{T}\sum_{n=-\infty}^{\infty} i[n - k - 1]p_{1,\tau}(t - nT),\\
e_{2,\tau}(t) &= \frac{1}{T}\sum_{n=-\infty}^{\infty} i[n - k]p_{2,\tau}(t - nT),\\
e_{3,\tau}(t) &= -\frac{1}{T}\sum_{n=-\infty}^{\infty} q[n - k - 1]p_{1,\tau}(t - nT),\\
e_{4,\tau}(t) &= -\frac{1}{T}\sum_{n=-\infty}^{\infty} q[n - k]p_{2,\tau}(t - nT).
\end{aligned} \tag{18}$$

It is now clear that

$$x_{m,k}[n] = \prod_{i \in S_m^1} i[n - k_i - 1] \cdot \prod_{i \in S_m^2} i[n - k_i] \cdot \prod_{i \in S_m^3} q[n - k_i - 1] \cdot \prod_{i \in S_m^4} q[n - k_i],$$

The input/output relation for system $\mathbf{DHF}_\tau\mathbf{M}$ readily follows from Lemma 2.2, and we have

$$v[n] = (\mathbf{A}u)[n],$$

where

$$u = \sum_{m\in[4]^d} x_{m,k} * g_{m,\tau},$$

and signals $x_{m,k}[n]$ are given by

$$x_{m,k}[n] = \prod_{i\in S_m^1} i[n-k_i-1] \cdot \prod_{i\in S_m^2} i[n-k_i] \cdot \prod_{i\in S_m^3} q[n-k_i-1] \cdot \prod_{i\in S_m^4} q[n-k_i],$$

and unit sample responses $g_{m,\tau}[n]$ have the following Fourier transforms

$$G_{m,\tau}(\Omega) = \sum_{r_c\in R_m^c} \sum_{r_s\in R_m^s} C_{r_c,r_s} P_{m,\tau}\left(\frac{\Omega}{T} - \omega_c \cdot \sigma(r) + \omega_c\right),$$

with C_{r_c,r_s} as given in (14).
This concludes the proof of Theorem 4.1. □

5 Discussion

5.1 Effects of oversampling

The potential significance of the result presented in this paper lies in revealing a special structure of a digital pre-distortion compensator which appears to be both necessary and sufficient to match the discrete time dynamics resulting from combining modulation and demodulation with a dynamic non-linearity in continuous time. The "necessity" somewhat relies on the input signal u having "full" spectrum. In digital communications it is very common practice to oversample baseband signal (symbols), and shape its spectrum (samples), before it is modulated onto a carrier [20]. In the case of large oversampling ratios, from symbol to sample space, the effective band of the signal containing symbol information is small compared to the band assigned by the regulatory agency. So in order to transmit symbol information without distortion, the reconstruction filter has to match the frequency response of the ideal baseband model LTI filter only on this effective band (and the rest can be zeroed-out by applying a smoothing filter after demodulation). This now allows for reconstruction filters in baseband equivalent model to be not just smooth, but also continuous, and thus well approximable by short memory FIR filters. This in turn implies that the plain Volterra structure with relatively short memory can capture dynamics of such system well enough, possibly diminishing the need for any special models. While, theoretically, the baseband signal u is supposed to be shaped so that only a lower DT frequency spectrum of it remains significant (i.e. oversampling is employed), a practical implementation of amplitude-phase modulation will frequently employ a signal component separation approach, such as LINC [21], where the low-pass signal u is decomposed into two

components of constant amplitude, $u = u_1 + u_2$, $|u_1[n]| \equiv |u_2[n]| = \text{const}$, after which the components u_i are fed into two separate modulators, to produce continuous time outputs y_1, y_2, to be combined into a single output $y = y_1 + y_2$. Even when u is band-limited, the resulting components u_1, u_2 are not, and the full range of modulator's nonlinearity is likely to be engaged when producing y_1 and y_2. Also in high-speed wideband communication systems, the oversampling ratio is usually limited by the speed that the digital baseband and DAC are able to sustain, therefore the latter scenario described is usually encountered and the compensator model should be able to take care of this factor.

5.2 Extension to OFDM

Orthogonal frequency-division multiplexing (OFDM) is a multicarrier digital modulation scheme that has been the dominant technology for broadband multicarrier communications in the last decade. Compared with single-carrier digital modulation, by increasing the effective symbol length and employing many carriers for transmission, OFDM theoretically eliminates the problem of multi-path channel fading, which is the main type of disturbance on a terrestrial transmission path. It also mitigates low spectrum efficiency, impulse noise, and frequency selective fading [20, 22]. One of the major drawbacks of OFDM is the relatively large Peak-to-Average Power Ratio (PAPR) [23]. This makes OFDM very sensitive to the nonlinear distortion introduced by high PA, which causes in-band as well as out-of-band (i.e. adjacent channel) radiation, decreasing spectral efficiency [24]. For that reason linearization techniques play very important role in OFDM, and have been studied extensively [25]-[27].

Figure 8. shows a block diagram of the typical implementation of an N-carrier OFDM system. Input stream of symbols $u[n]$, with bandwidth B, is first converted into blocks of lenght N by serial-to-parallel conversion, which are then fed to an N-point inverse FFT block. Output of this block is then transformed with a parallel-to-serial converter into a stream of N samples $v[k]$, with bandwidth B (usually this bandwidth is larger than the input symbols' bandwidth, but in our discussion we ignore introduction of the guard interval (i.e. addition of cyclic redundancy), which is usually used to mitigate the impairments of the multipath radio channel, as it does not affect aplicability of the baseband model and the DPD proposed in this paper). Digital-to-analog convertion is then applied to $v[k]$, and its output is used to modulate a single carrier. As can be seen from Figure 8, sequence $v[k]$ can be seen as an input to a system which can be modeled as the $\mathbf{DHFM}$ system investigated in the previous chapter. In our derivation of the baseband model, choice of the input symbols' values (e.g. QPSK, QAM, etc.), was not relevant to the actual derivation. In other words, input symbols can take any value from $\mathbb{C}$, hence sequence $v[k]$ can be considered as a legitimate input sequence to a system modeled as $\mathbf{DHFM}$. This suggests that our baseband model, and its corresponding DPD structure, can be possibly used for distortion reduction in OFDM modulation applications.

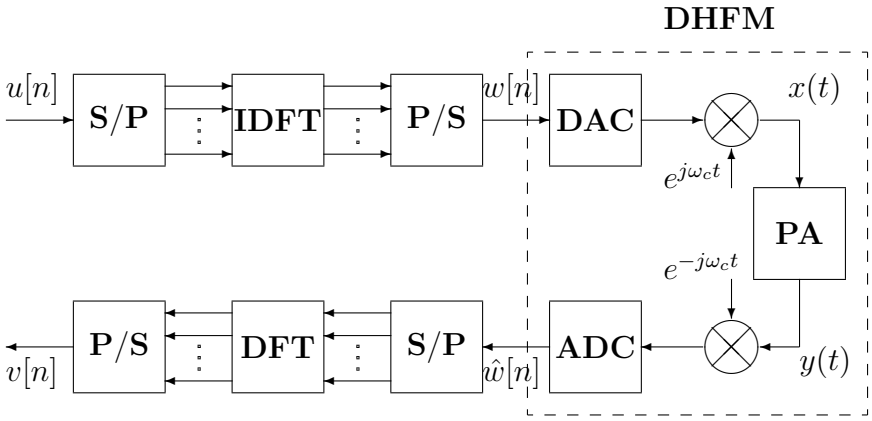

Figure 8: Block diagram of the typical implementation of OFDM

6 Simulation Results

In this section, through MATLAB simulations, we illustrate performance of the proposed compensator structure. We compare this structure with some standard compensator structures, together with ideal compensator, and show that it closely resembles dynamics of ideal compensator, thus achieving very good compensation performance.
The underlying system $\mathbf{S}$ is given in Figure 1, with the distortion subsystem $\mathbf{F}$ given by

$$(Fx)(t) = x(t) - \delta \cdot x(t-\tau_1)x(t-\tau_2)x(t-\tau_3), \tag{19}$$

where $0 \leq \tau_1 \leq \tau_2 \leq \tau_3 \leq T$, with T sampling time, and $\delta > 0$ parameter specifying magnitude of distortion $\mathbf{\Delta}$ in $\mathbf{S} = \mathbf{I} + \mathbf{\Delta}$. We assume that parameter δ is relatively small, in particular $\delta \in (0, 0.2)$, so that the inverse $\mathbf{S}^{-1}$ of $\mathbf{S}$ can be well approximated by $2\mathbf{I} - \mathbf{S}$. Then our goal is to build compensator $\mathbf{C} = \mathbf{S}^{-1}$ with different structures, and compare their performance, which is measured as output Error Vector Magnitude (EVM) [3]. EVM, for an input u and output $\hat{u}$, is defined as

$$\text{EVM(dB)} = 20\log_{10}\left(\frac{||u-\hat{u}||_2}{||u||_2}\right).$$

Analytical results from the previous section suggest that the compensator structure should be of the form depicted in Figure 2. It is easy to see from the proof of Theorem 4.1, that transfer functions in $\mathbf{L}$, from each nonlinear component $g_k[n]$ of $g[n]$, to the output $v[n]$, are smooth functions, hence can be well approximated by low order polynomials in Ω. In this example we choose second order polynomial approximation of components of $\mathbf{L}$. This observation, together with the true structure of $\mathbf{S}$, suggests that compensator $\mathbf{C}$ should be fit within a family of models with structure shown on the block diagram in Fig 9.

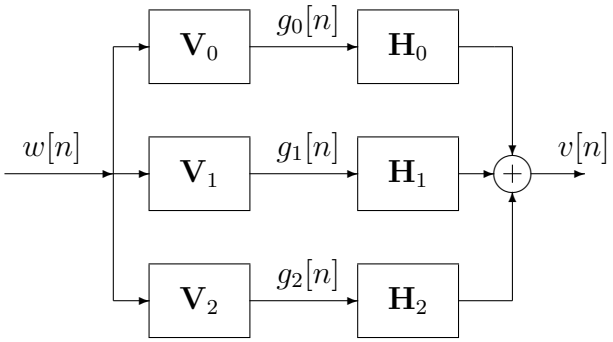

Figure 9: Proposed compensator structure

Subsystems $\mathbf{H}_i, i = 1, 2, 3$, are LTI systems, with transfer functions H_i given by

$$H_0(e^{j\Omega}) = 1, H_1(e^{j\Omega}) = j\Omega, H_2(e^{j\Omega}) = \Omega^2, \forall\Omega \in [-\pi, \pi].$$

Nonlinear subsystems $\mathbf{V}_i$ are modeled as third order Volterra series, with memory $m = 1$, i.e.

$$(\mathbf{V}_j w)[n] = \sum_{(\alpha(k),\beta(k))} c_k^j \prod_{l=0}^{1} i[n-l]^{\alpha_l(k)} \prod_{l=0}^{1} q[n-l]^{\beta_l(k)},$$

$$\alpha_l(k), \beta_l(k) \in \mathbb{Z}_+, \qquad \sum_{l=0}^{1} \alpha_l(k) + \sum_{l=0}^{1} \beta_l(k) \leq 3,$$

where $i[n] = \mathrm{R}e\ w[n]$ and $q[n] = \mathrm{I}m\ w[n]$, and $(\alpha(k), \beta(k)) = (\alpha_0(k), \alpha_1(k), \beta_0(k), \beta_1(k))$.

We compare performance of this compensator with the widely used one obtained by utilizing simple Volterra series structure [3]:

$$(\mathbf{C}w)[n] = \sum_{(\alpha(k),\beta(k))} c_k \prod_{l=-m_1}^{m_2} i[n-l]^{\alpha_l(k)} \prod_{l=-m_1}^{m_2} q[n-l]^{\beta_l(k)},$$

$$\alpha_l(k), \beta_l(k) \in \mathbb{Z}_+, \qquad \sum_{l=-m_1}^{m_2} \alpha_l(k) + \sum_{l=-m_1}^{m_2} \beta_l(k) \leq d.$$

Parameters which could be varied in this case are forward and backward memory depth m_1 and m_2, respectively, and degree d of this model. We consider three cases for different sets of parameter values:

- Case 1: $m_1 = 0,\ m_2 = 2,\ d = 5$
- Case 2: $m_1 = 0,\ m_2 = 4,\ d = 5$
- Case 3: $m_1 = 2,\ m_2 = 2,\ d = 5$

Table 1: Number of coefficients c_k being optimized for different compensator models

Model	# of c_k	# of significant c_k
New structure	210	141
Volterra 1	924	177
Volterra 2	6006	2058
Volterra 3	6006	1935

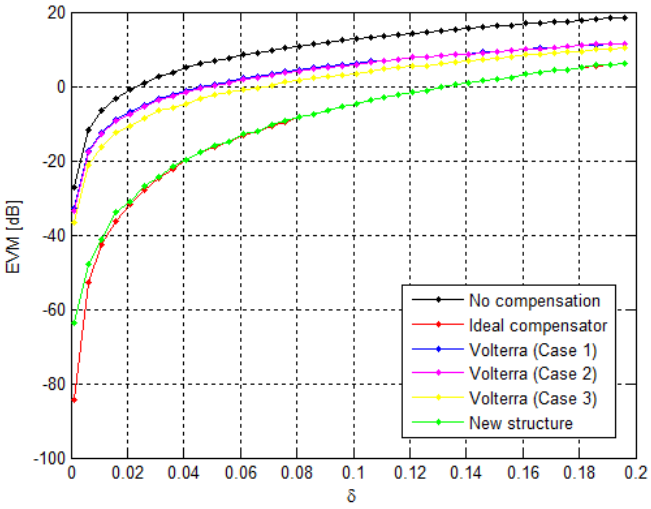

Figure 10: Output EVM for different compensator structures

After fixing compensator structure, coefficients c_k are obtained by applying straightforward least squares optimization.
We should emphasize here that fitting has to be done for both real and imaginary part of $v[n]$, thus the actual compensator structure is twice that depicted in Figure 9.

Simulation parameters for system $\mathbf{S}$ are as follows: symbol rate $f_{symb} = 2$MHz, carrier frequency $f_c = 20$MHz, with 64QAM input symbol sequence. Nonlinear distortion subsystem $\mathbf{F}$ of $\mathbf{S}$, used in simulation, is defined in (19), where the delays τ_1, τ_2, τ_3 are given by the vector $\tau = [0.2T \quad 0.3T \quad 0.4T]$, with $T = 1/f_{symb}$. Digital simulation of the continuous part of $\mathbf{S}$ was done by representing continuous signals by their discrete counterparts, obtained by sampling with high sampling rate $f_s = 1000 \cdot f_{symb}$. As input to $\mathbf{S}$, we assume periodic 64QAM symbol sequence, with period $N_{symb} = 4096$. This period length is used for generating input/output data for fitting coefficients c_k, as well as generating input/output data for performance validation.
In Figure 10 we present EVM obtained for different compensator structures, as well as output EVM with no compensation, and case with ideal compensator $\mathbf{C} = \mathbf{S}^{-1} \approx 2\mathbf{I} - \mathbf{S}$. As can be seen from Figure 10, compensator fitted using the proposed structure in Figure 9 outperforms

other compensators, and gives output EVM almost identical to the ideal compensator. This result was to be expected, since model in Figure 9 approximates the original system $\mathbf{S}$ very closely, and thus is capable of approximating system $2\mathbf{I} - \mathbf{S}$ closely as well. This is not the case for compensators modeled with simple Volterra series, due to inherently long (or more precisely infinite) memory introduced by the LTI part of $\mathbf{S}$. Even if we use noncausal Volterra series model (i.e. $m_1 \neq 0$), which is expected to capture true dynamics better, we are still unable to get good fitting of the system $\mathbf{S}$, and consequently of the compensator $\mathbf{C} \approx 2\mathbf{I} - \mathbf{S}$.
Advantage of the proposed compensator structure is not only in better compensation performance, but also in that it achieves better performance with much more efficient strucuture. That is, we need far less coefficients in order to represent nonlinear part of the compensator, in both least squares optimization and actual implementation (Table 1). In Table 1 we can see a comparison in the number of coefficients between different compensator structures, for nonlinear subsystem parameter value $\delta = 0.02$. Data in the first column is number of coefficients (i.e. basis elements) needed for general Volterra model, i.e. coefficients which are optimized by least squares. The second column shows actual number of coefficients used to build compensator. Least squares optimization yields many nonzero coefficients, but only subset of those are considered significant and thus used in actual compensator implementation. Coefficient is considered significant if its value falls above a certain treshold t, where t is chosen such that increase in EVM after zeroing nonsignificant coefficients is not larger than 1% of the best achievable EVM (i.e. when all basis elements are used for building compensator). From Table 1 we can see that for case 3 Volterra structure, 10 times more coefficients are needed in order to implement compensator, than in the case of our proposed structure. And even when such a large number of coefficients is used, its performance is still below the one achieved by this new compensator model.

7 Conclusion

In this paper, we propose a novel explicit expression of the equivalent baseband model, under assumption that the passband nonlinearity can be described by a Volterra series model with the fixed degree and memory depth. This result suggests a new, non-obvious, analytically motivated structure of digital precompensation of passband nonlinear distortions caused by power amplifiers, in digital communication systems. It has been shown that the baseband equivalent model can be written as a series connection of a fixed degree and low memory Volterra model, and a long memory discrete LTI system, called reconstruction filter. Frequency response of the reconstruction filter is shown to be smooth, hence well aproximable by low order polynomials. Parameters of such a model (and accordingly of the predistorter) can be obtained by applying simple least squares optimization to the input/output data measured from the system, thus implying low implementation complexity. State of the art implementations of DPD, have long memory requirements in the nonlinear subsystem, but structure of our baseband equivalent model suggests that the long memory requirements are shifted from the nonlinear part, to the LTI part, which consists of FIR filters and is easy to implement in digital circuits, giving it advantage of much lower complexity. We also argued that this baseband model, and its cor-

responding DPD structure, can be readily extended to OFDM modulation. Simulation results have shown that by using this new DPD structure, significant reduction in nonlinear distortion caused by the RF PA can be achieved, while utilizing full frequency band, and thus effectively using maximal input symbol rate.

Acknowledgment

The authors are grateful to Dr. Yehuda Avniel for bringing researchers from vastly different backgrounds to work together on the tasks that led to the writing of this paper.

References

[1] P. B. Kennington, *High linearity RF amplifier design*. Norwood, MA: Artech House, 2000.

[2] S. C. Cripps, *Advanced techniques in RF power amplifier design*. Norwood, MA: Artech House, 2002.

[3] J. Vuolevi, and T. Rahkonen, *Distortion in RF Power Amplifiers*. Norwood, MA: Artech House, 2003.

[4] A. A. M. Saleh, and J. Salz, "Adaptive linearization of power amplifiers in digital radio systems," *Bell Syst. Tech. J.*, vol. 62, no. 4, pp. 1019-1033, April 1983.

[5] W. Bösch, and G. Gatti, "Measurement and simulation of memory effects in predistortion linearizers," *IEEE Trans. Microw. Theory Techn.*, vol. 37, pp. 1885-1890, December 1989.

[6] J. Kim, and K. Konstantinou, "Digital predistortion of wideband signals based on power amplifier model with memory," *Electron. Lett.*, vol 37, no. 23, pp. 1417-1418, November 2001.

[7] L. Ding, G. T. Zhou, D. R. Morgan, Z. Ma, J. S. Kenney, J. Kim, and C. R. Giardina, "A robust digital baseband predistorter constructed using memory polynomials," *IEEE Trans. Commun.*, vol. 52, no. 1, pp.159-165, January 2004.

[8] V. J. Mathews and G. L. Sicuranza, *Polynomial Signal Processing*. New York: Wiley, 2000.

[9] A. Zhu, and T. Brazil, "Behavioral modeling of RF power amplifiers based on pruned Volterra series," *IEEE Microw. Wireless Compon. Lett.*, vol. 14, no. 12, pp. 563-565, December 2004

[10] D. R. Morgan, Z. Ma, J. Kim, M. Zierdt, and J. Pastalan, "A generalized memory polynomial model for digital predistortion of RF power amplifiers," *IEEE Trans. Signal Process.*, vol. 54, no. 10, pp. 3852-3860, October 2006.

[11] A. Zhu, J. C. Pedro, and T. J. Brazil, "Dynamic deviation reduction-based Volterra behavioral modeling of RF power amplifiers," *IEEE Trans. Microw. Theory Techn.*, vol. 54, No. 12, pp. 4323-4332., December 2006.

[12] A. Zhu, P. J. Draxler, J. J. Yan, T. J. Brazil, D. F. Kimball, and P. M. Asbeck, "Open-loop digital predistorter for RF power amplifiers using dynamic deviation reduction-based Volterra series," *IEEE Trans. Microw. Theory Techn.*, vol. 56, No. 7, pp. 1524-1534., July 2008.

[13] M. Rawat, K. Rawat, and F. M. Ghannouchi, "Adaptive digital predistortion of wireless power amplifiers/transmitters using dynamic real-valued focused time-delay line neural networks," *IEEE Trans. Microw. Theory Techn.*, vol. 58, No. 1, pp. 95-104, January 2010.

[14] M. Rawat, K. Rawat, F. M. Ghannouchi, S. Bhattacharjee, and H. Leung, "Generalized rational functions for reduced-complexity behavioral modeling and digital predistortion of broadband wireless transmitters," *IEEE Trans. Instrum. Meas.*, vol. 63, No. 2, pp. 485-498, February 2014.

[15] C. Yu, L. Guan, and A. Zhu, "Band-Limited Volterra Series-Based Digital Predistortion for Wideband RF Power Amplifiers," *IEEE Trans. Microw. Theory Techn.*, vol. 60, No. 12, pp. 4198-4208, December 2012.

[16] G. M. Raz, and B. D. Van Veen, "Baseband Volterra filters for implementing carrier based nonlinearities," *IEEE Trans. Signal Process.*, vol. 46, no. 1, pp. 103-114, January 1998.

[17] M. Schetzen, *The Volterra and Wiener theories of nonlinear systems*. reprint ed. Malabar, FL: Krieger, 2006.

[18] W. Frank, "Sampling requirements for Volterra system identification," *IEEE Signal Process. Lett.*, vol. 3, no. 9, pp. 266-268, September 1996

[19] J.Tsimbinos, and K.V.Lever, "Input Nyquist sampling suffices to identify and compensate nonlinear systems," *IEEE Trans. Signal Process.*, vol. 46, no. 10, pp. 2833-2837, Oct. 1998.

[20] J. G. Proakis and M. Salehi, *Digital Communications*. McGraw-Hill, 2007

[21] D. C. Cox, "Linear amplification with nonlinear components," *IEEE Trans. Commun.*, vol. 22, no. 12, pp. 1942-1945, Dec. 1974.

[22] A. Goldsmith, *Wireless Communications*. Cambridge University Press, 2005.

[23] S. H. Han and J. H. Lee, "An overview of peak-to-average power ratio reduction techniques for multicarrier transmission," *IEEE Wireless Commun.*, vol. 52, pp. 5-65, March 2005

[24] Q. Shi, "OFDM in bandpass nonlinearity," *IEEE Trans. Consumer Electron.*, vol. 42, pp. 253-258, August 1996.

[25] A. N. D'Andrea, V. Lottici, and R. Reggiannini, "Nonlinear predistortion of OFDM signals over frequency-selective fading channels," *IEEE Trans. Commun.*, vol. 49, no. 5, pp. 837-843, May 2001.

[26] F. Wang; D.F. Kimball, D.Y. Lie, P.M. Asbeck, and L. E. Larson, "A Monolithic High-Efficiency 2.4-GHz 20-dBm SiGe BiCMOS Envelope-Tracking OFDM Power Amplifier," *IEEE J. Solid-State Circuits*, vol.42, no.6, pp.1271,1281, June 2007.

[27] J. Reina-Tosina, M. Allegue-Martinez, C. Crespo-Cadenas, C. Yu, and S. Cruces, "Behavioral Modeling and Predistortion of Power Amplifiers Under Sparsity Hypothesis," *IEEE Trans. Microw. Theory Techn.*, vol. 63, no. 2, pp. 745-753, February 2015.

[28] O. Tanovic, A. Megretski, Y. Li ,V. Stojanovic, and M. Osqui, "Discrete-Time Models Resulting From Dynamic Continuous-Time Perturbations In Phase-Amplitude Modulation-Demodulation Schemes," *Proceedings of the European Control Conference 2015*, pp. 3571-3576, July 15-17, 2015.